604 *Inorg. Chem.* **2011**, *50*, 604–613
DOI: 10.1021/ic101672t

Inorganic Chemistry
Article

Self-Assembly of Hybrid Organic−Inorganic Polyoxomolybdates: Solid-State Structures and Investigation of Formation and Core Rearrangements in Solution

Camelia I. Onet,[†] Lei Zhang,[†] Rodolphe Clérac,[‡,§] J. Bernard Jean-Denis,[†] Martin Feeney,[†] Thomas McCabe,[†] and Wolfgang Schmitt*[,†]

[†]*School of Chemistry, Trinity College, The University of Dublin, Dublin 2, Ireland,* [‡]*Centre de Recherche Paul Pascal (CRPP), Equipe "Matériaux Moléculaires Magnétiques", CNRS, UPR 8641, 115 avenue du Dr. Albert Schweitzer, Pessac F-33600, France, and* [§]*Université de Bordeaux, UPR 8641, Pessac F-33600, France*

Received August 17, 2010

We report here a facile synthetic and analytical approach that allows us to identify and characterize functionalized polyoxomolybdate clusters that form upon the partial reduction of Mo^{VI} salts in the presence of organoarsonate ligands. We demonstrated that electrospray ionization mass spectrometry, in combination with X-ray crystallography, provides an extremely powerful tool, allowing us to exploit slight perturbations of the ligand structures for the preparation of a series of unprecedented cluster compounds. Redox-active transition metals that adopt cubane or related structures are of particular interest because of their resemblance to active sites of enzymes. Our investigations underline the stability of the hybrid compounds in solution, an essential requirement for potential applications as catalysts. Supplemental analyses include measurements of the magnetic properties, NMR, IR, UV/vis, and bond-valence-sum analyses. Our results highlight the possibility of exploring real-time growth reactions of polyoxometales that emerge in solution and transform to produce hybrid organic−inorganic polyoxometalate clusters.

Introduction

The chemistry of polyoxometalates (POMs) is one of the most active and rapidly advancing areas of inorganic chemistry.[1,2] The interest in the oxo clusters of the early-transition-metal ions is based on their unique structural characteristics and chemical attributes (including redox and photochemical activity and optical properties, charge distribution, and band structures), which promote applications as catalysts, sensors, photocatalysts, electrochromic materials, energy storage, and conversion devices.[2,3] Their reactions in aqueous solution and the resulting structures can often be rationalized by aggregations of small molecular species, producing oligomeric complexes, large nanoscale clusters, or infinite oxides.[4,5] The early-transition-metal ions are able to polarize terminal M−O bonds stabilizing large molecular cage structures and other aggregates. However, these bonds, which are characterized by d−π contributions and reveal significant double-bond character, also impede functionalization. Functionalization approaches to generate hybrid POM structures or advanced inorganic materials remain an ongoing challenge, and new synthetic and analytical approaches are pivotal to the progress of the field.[1,6] We are interested in the chemistry

*To whom correspondence should be addressed. E-mail: schmittw@tcd.ie. Tel: +353 1 896 3495. Fax: +353 1 671 2826.

(1) (a) Proust, A.; Thouvenot, R.; Gouzerh, P. *Chem. Commun.* **2008**, 1837–1852. (b) Gouzerh, P.; Proust, A. *Chem. Rev.* **1998**, *98*, 77–111. (c) Long, D.-L.; Cronin, L. *Chem.—Eur. J.* **2006**, *12*, 3698–3706.

(2) (a) Dey, K. C.; Sharma, V. *Int. J. ChemTech Res.* **2010**, *2*, 368–375. (b) Qi, W.; Wang, Y.; Li, W.; Wu, L. *Chem.—Eur. J.* **2010**, *16*, 1068–1078. (c) Wang, M.-S.; Xu, G.; Zhang, Z.-J.; Guo, G.-C. *Chem. Commun.* **2010**, *46*, 361–376. (d) Wang, Z.; Zhang, R.; Ma, Y.; Peng, A.; Fua, H.; Yao, J. *J. Mater. Chem.* **2010**, *20*, 271–277. (e) Wang, Z.; Zhang, R.; Ma, Y.; Zheng, L.; Peng, A.; Fua, H.; Yao, J. *J. Mater. Chem.* **2010**, *20*, 1107–1111. (f) Saraiva, M. S.; Gamelas, J. A. F.; Mendes de Sousa, A. P.; Reis, B. M.; Amaral, J. L.; Ferreira, P. J. *Materials* **2010**, *3*, 201–215. (g) Fernandes, D. M.; Simões, S. M. N.; Carapuça, H. M.; Brett, C. M. A.; Cavaleiro, A. M.V. *J. Electroanal. Chem.* **2010**, *639*, 83–87. (h) Prudent, R.; Sautel, C. F.; Cochet, C. *Biochim. Biophys. Acta* **2010**, *1804*, 493–498. (i) Zheng, L.; Ma, Y.; Zhang, G.; Yao, J.; Keita, B.; Nadjoc, L. *Phys. Chem. Chem. Phys.* **2010**, *12*, 1299–1304.

(3) (a) Müller, A.; Kögerler, P.; Kuhlmann, C. *Chem. Commun.* **1999**, 1347–1358. (b) Long, D.-L.; Burkholder, E.; Cronin, L. *Chem. Soc. Rev.* **2007**, *36*, 105–121. (c) Kortz, U.; Müller, A.; van Slageren, J.; Schnack, J.; Dalal, N. S.; Dressel, M. *Coord. Chem. Rev.* **2009**, *253*, 2315–2327. (d) Katsoulis, D. E. *Chem. Rev.* **1998**, *98*, 359–387. (e) Mizuno, N.; Misono, M. *Chem. Rev.* **1998**, *98*, 199–217. (f) Yamase, T. *Chem. Rev.* **1998**, *98*, 307–325. (g) Kozhevnikov, I. V. *Chem. Rev.* **1998**, *98*, 171–198. (h) Rhule, J. T.; Neiwert, W. A.; Hardcastle, K. I.; Do, B. T.; Hill, C. L. *J. Am. Chem. Soc.* **2001**, *123*, 12101–12102. (i) Müller, A.; Luban, M.; Schröder, C.; Modler, R.; Kögerler, P.; Axenovich, M.; Schnack, J.; Canfield, P.; Bud'ko, S.; Harrison, N. *ChemPhysChem* **2001**, *2*, 517–521.

(4) (a) Müller, A.; Beckmann, E.; Bögge, H.; Schmidtmann, M.; Dress, A. *Angew. Chem., Int. Ed.* **2002**, *41*, 1162–1167. (b) Ismail, A. H.; Bassil, B. S.; Suchopar, A.; Kortz, U. *Eur. J. Inorg. Chem.* **2009**, 5247–5252. (c) Mal, S. S.; Bassil, B. S.; Ibrahim, M.; Nellutla, S.; Tol, J.; Dalal, N. S.; Fernandez, J. A.; Lopez, X.; Poblet, J. M.; Biboum, R. N.; Keita, B.; Kortz, U. *Inorg. Chem.* **2009**, *48*, 11636–11645. (d) Bassil, B. S.; Dickman, M. H.; Römer, I.; Kammer, B.; Kortz, U. *Angew. Chem., Int. Ed.* **2007**, *46*, 6192–6195.

(5) Cronin, L. High Nuclearity Polyoxometalate Clusters. In *Comprehensive Coordination Chemistry II*; McLeverty, J. A., Meyer, T. J., Eds.; Elsevier Publishers: Amsterdam, The Netherlands, 2004; Vol. *7*, pp 1−57.

(6) Mialane, P.; Dolbecq, A.; Sécheresse, F. *Chem. Commun.* **2006**, 3477–3485.

Published on Web 12/08/2010

of hybrid organic−inorganic materials,[7] and we decided to explore the formation of mixed-valent molybdates in the presence of organoarsonates and -phosphonates. Phosphonate- and arsonate-stabilized oxo clusters that contain redox-active metal centers are of interest for applications in catalysis.[3c−g] The geometrical characteristics of the functional groups of the organophosphonates and -arsonates might promote the formation of structures that enhance the electrochemical splitting of water and reduce overpotentials when deposited on electrodes.[8] Several organoarsonate-stabilized polyoxomolybdates of varying nuclearity and containing different core structures have been reported. Examples include $Mo_4O_{10}(O_3AsR)_4\}^{4-}$, $\{Mo_6O_{12}(O_3AsR)\}^{4+}$, $\{Mo_6O_{18}(O_3AsR)_2\}^{4-}$, and $\{Mo_{12}O_{34}(O_3AsR)_4\}^{4-}$ (R = CH_3, C_6H_5, $C_6H_4CH_3$, C_6H_4-4-NH_2, C_6H_4-4-OH, C_6H_4-4-COOH, C_6H_3-4-OH-3-NO_2, C_6H_4-4-CN, C_6H_3-4-OH-3-NOC_2H_4).[9a−l]

Despite an ever-increasing interest in POM complexes, it is surprising that their solution behavior, i.e., formation reactions that often prevail through a set of consecutive condensation reactions, is often fairly poorly understood. However, speciation within POM solutions not only is important to devise rational synthetic approaches to desired products but is, moreover, a prerequisite to improve catalytic processes that draw on the active sites or electronic characteristics of POMs. Recent accounts demonstrate that electrospray ionization mass spectrometry (ESI-MS) provides a very powerful analytical tool to characterize the formation and reactivity of complex POM clusters in solution.[10]

Scheme 1. Organoarsonic Acids Used in These Studies: Phenylarsonic Acid (PAA), 4-Aminophenylarsonic Acid (APAA), 4-Hydroxyphenylarsonic Acid (HPAA), 4-Hydroxy-3-nitrophenylarsonic Acid (HNPAA)

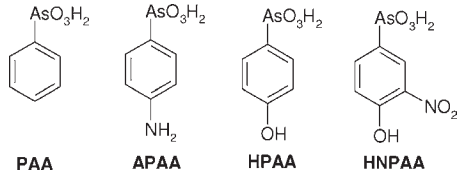

Results and Discussion

We decided to use ESI-MS to investigate the self-assembly process of hybrid polyoxomolybdates that form upon the partial reduction of $(NH_4)_6Mo_7O_{24}\cdot 4H_2O$ in the presence of aromatic organoarsonates (Scheme 1). We were interested in exploring how perturbations of the ligand functionality influence the formation of unprecedented species. Although several arsonate-stabilized molybdates had previously been reported,[9] mass spectrometry allowed us to selectively identify species with unprecedented core structures. Here we report the solution characterization, structures, and properties of four hybrid cluster anions that self-assemble under these reaction conditions: $[Mo^V_4O_8(O_3AsC_6H_5)_4]^{4-}$ (**1**), $[Mo^V_4O_8(O_3AsC_6H_4NH_2)_4]^{4-}$ (**2**), $[Mo^{VI}_2Mo^V_3O_{11}(O_3AsC_6H_4OH)_5]^{5-}$ (**3**), and $[Mo^{VI}_4O_{10}(O_3AsC_6H_3NO_2OH)_4]^{4-}$ (**4**). Utilizing ESI-MS during the screening process of the reaction mixtures, we could identify new species whose structures and composition were later confirmed by standard single-crystal X-ray diffraction studies. A summary of the assignments of the ESI-MS spectra and the experimental conditions is given in the Supporting Information (Table S5). Further supplemental analyses include NMR spectroscopy, elemental analysis, magnetic studies, thermogravimetric analyses, powder X-ray diffraction, and bond-valence-sum analyses.

Phenylarsonic Acid (PAA)−Mo^{VI}/Mo^V Reaction System. The partial reduction of $(NH_4)_6Mo_7O_{24}\cdot 4H_2O$ in the presence of PAA and acetic acid using $N_2H_4\cdot H_2SO_4$ results in a deep-blue solution. When the initial reaction mixture is examined by ESI-MS, the spectrum reveals isotopic envelopes in the high-molecular-mass region centered at m/z 1315.3 and 1659.2 (Figure 1). Within a time period of 3 weeks, dark-red crystals of $(NH_4)_2H_2$[**1**]$\cdot 5H_2O$ separate from this reaction mixture.

Single-crystal X-ray analysis reveals that **1** contains a tetranuclear molybdenum complex in which the Mo atoms and bridging O donors adopt a typical $[Mo_4(\mu_3\text{-}O)_4]^{12+}$

(7) (a) Breen, J. M.; Schmitt, W. *Angew. Chem., Int. Ed.* **2008**, *47*, 6904–6908. (b) La Spina, G.; Clérac, R.; Collins, E. S.; McCabe, T.; Venkatesan, M.; Ichinose, I.; Schmitt, W. *Dalton Trans.* **2007**, 5248–5252. (c) Schmitt, W.; Anson, C. E.; Hill, J. P.; Powell, A. K. *J. Am. Chem. Soc.* **2003**, *125*, 11142–11143. (d) Schmitt, W.; Hill, J. P.; Juanico, M. P.; Caneschi, A.; Costantion, F.; Anson, C. E.; Powell, A. K. *Angew. Chem., Int. Ed.* **2005**, *44*, 4187–4192. (e) McKeogh, I.; Hill, J. P.; Collins, E. S.; McCabe, T.; Powell, A. K.; Schmitt, W. *New J. Chem.* **2007**, *31*, 1882–1885. (f) Schmitt, W.; Anson, C. E.; Pilawa, B.; Powell, A. K. *Z. Anorg. Allg. Chem.* **2002**, *628*, 2443–2452. (g) Schmitt, W.; Hill, J. P.; Malik, S.; Volkert, C. A.; Ichinose, I.; Anson, C. E.; Powell, A. K. *Angew. Chem., Int. Ed.* **2005**, *44*, 7048–7053.

(8) (a) Kanan, M. W.; Nocera, D. G. *Science* **2008**, *321*, 1072–1075. (b) Kanan, M. W.; Surendranath, Y.; Nocera, D. G. *Chem. Soc. Rev.* **2009**, *38*, 109–114. (c) Surendranath, Y.; Dinca, M.; Nocera, D. G. *J. Am. Chem. Soc.* **2009**, *131*, 2615–2620. (d) Lutterman, D. A.; Surendranath, Y.; Nocera, D. G. *J. Am. Chem. Soc.* **2009**, *131*, 3838–3839. (e) Barber, J. *Philos. Trans. R. Soc. A* **2007**, *365*, 1007–1023. (f) Barber, J. *Inorg. Chem.* **2008**, *47*, 1700–1710. (g) Carrell, T. G.; Bourles, E.; Lin, M.; Dismukes, G. C. *Inorg. Chem.* **2003**, *42*, 2849–2858. (h) Rothger, D. W.; Mann, J. E.; Jarrold, C. C. *J. Chem. Phys.* **2010**, *133*, 054305/1–054305/10. (i) Karunadasa, H. I.; Chang, C. J.; Long, J. R. *Nature* **2010**, *464*, 1329–1333. (j) Eisenberg, R.; Gray, H. B. *Inorg. Chem.* **2008**, *47*, 1697–1699.

(9) (a) Dolbecq, A.; Compain, J.-D.; Mialane, P.; Marrot, J.; Sécheresse, F.; Keita, B.; Holzle, L. R. B.; Miserque, F.; Nadjo, L. *Chem.—Eur. J.* **2009**, *15*, 733–741. (b) Tan, S.; Hobday, M.; Gorman, J.; Amiet, G.; Rix, C. *J. Mater. Chem.* **2003**, *13*, 1180–1185. (c) You, X. Z.; Li, H. L. *Acta Crystallogr.* **1993**, *49*, 1300–1303. (d) Johnson, B. J. S.; Buss, C. E.; Young, V. G.; Stein, A. *Acta Crystallogr.* **1999**, *55*, 549–551. (e) Matsumoto, K. Y. *Bull. Chem. Soc. Jpn.* **1978**, *51*, 492–498. (f) Chang, Y.-D.; Zubieta, J. *lnorg. Chim. Acta* **1996**, *245*, 177–198. (g) Burkholder, E.; Zubieta, J. *Inorg. Chim. Acta* **2004**, *357*, 301–304. (h) Johnson, B. J. S.; Schroden, R. C.; Zhu, C.; Stein, A. *Inorg. Chem.* **2001**, *40*, 5972–5978. (i) Barkigia, K. M.; Rajkovic-Blazer, L. M.; Pope, M. T.; Quicksall, C. O. *Inorg. Chem.* **1981**, *20*, 3318–3323. (j) Klemperer, W. G.; Schwartz, C.; Wright, D. A. *J. Am. Chem. Soc.* **1985**, *107*, 6941–6950. (k) Burkholder, E.; Wright, S.; Golub, V.; O'Connor, C. J.; Zubieta, J. *Inorg. Chem.* **2003**, *42*, 7460–7471. (l) Johnson, B. J. S.; Schroden, R. C.; Zhu, C.; Young, V. G.; Stein, A. *Inorg. Chem.* **2002**, *41*, 2213–2218. (m) Johnson, B. J. S.; Geers, S. A.; Brennessel, W. W.; Young, V. G., Jr.; Stein, A. *Dalton Trans.* **2003**, 4678–4681. (n) Kwak, W.; Rajkovic, L. M.; Stalick, J. K.; Pope, M. T.; Quicksall, C. O. *Inorg. Chem.* **1976**, *15*, 2778–2783. (o) Kwak, W.; Rajkovic, L. M.; Pope, M. T.; Quicksall, C. O.; Matsumoto, K. Y.; Sasaki, Y. *J. Am. Chem. Soc.* **1977**, *99*, 6463–6464. (p) Johnson, B. J. S.; Schroden, R. C.; Zhu, C.; Stein, A. *Inorg. Chem.* **2001**, *40*, 5972–5978.

(10) (a) Miras, H. N.; Wilsonw, E. F.; Cronin, L. *Chem. Commun.* **2009**, 1297–1311. (b) Wilson, E. F.; Abbas, H.; Duncombe, B. J.; Streb, C.; Long, D.-L.; Cronin, L. *J. Am. Chem. Soc.* **2008**, *130*, 13876–13884. (c) Tsunashima, R.; Long, D.-L.; Miras, H. N.; Gabb, D.; Pradeep, C. P.; Cronin, L. *Angew. Chem., Int. Ed.* **2010**, *49*, 113–116. (d) Song, Y.; Long, D.-L.; Kelly, S. E.; Cronin, L. *Inorg. Chem.* **2008**, *47*, 9137–9139. (e) Tuoi, J. L. Q.; Muller, E. *Rapid. Commun. Mass Spectrosc.* **1994**, *8*, 692–694. (f) Ma, M. T.; Waters, T.; Beyer, K.; Palamarczuk, R.; Richardt, P. J. S.; Hair, R. A. J.; Wedd, A. G. *Inorg. Chem.* **2009**, *48*, 598–606. (g) Bonchio, M.; Bortolini, O.; Conte, V.; Sartorel, A. *Eur. J. Inorg. Chem.* **2003**, 699–704. (h) Walanda, D. K.; Burns, R. C.; Lawrance, G. A.; Nagy-Felsobuki, E. I. *J. Chem. Soc., Dalton. Trans.* **1999**, 311–321. (i) Sahureka, F.; Burns, R. C.; Nagy-Felsobuki, E. I. *J. Inorg. Chim. Acta* **2003**, *351*, 69–78. (j) Deery, M. J.; Howarth, O. W.; Jennings, K. R. *J. Chem. Soc., Dalton Trans.* **1997**, 4783–4788. (k) Llusar, R.; Sorribes, I.; Vicent, C. *J. Cluster Sci.* **2009**, *20*, 177–192.

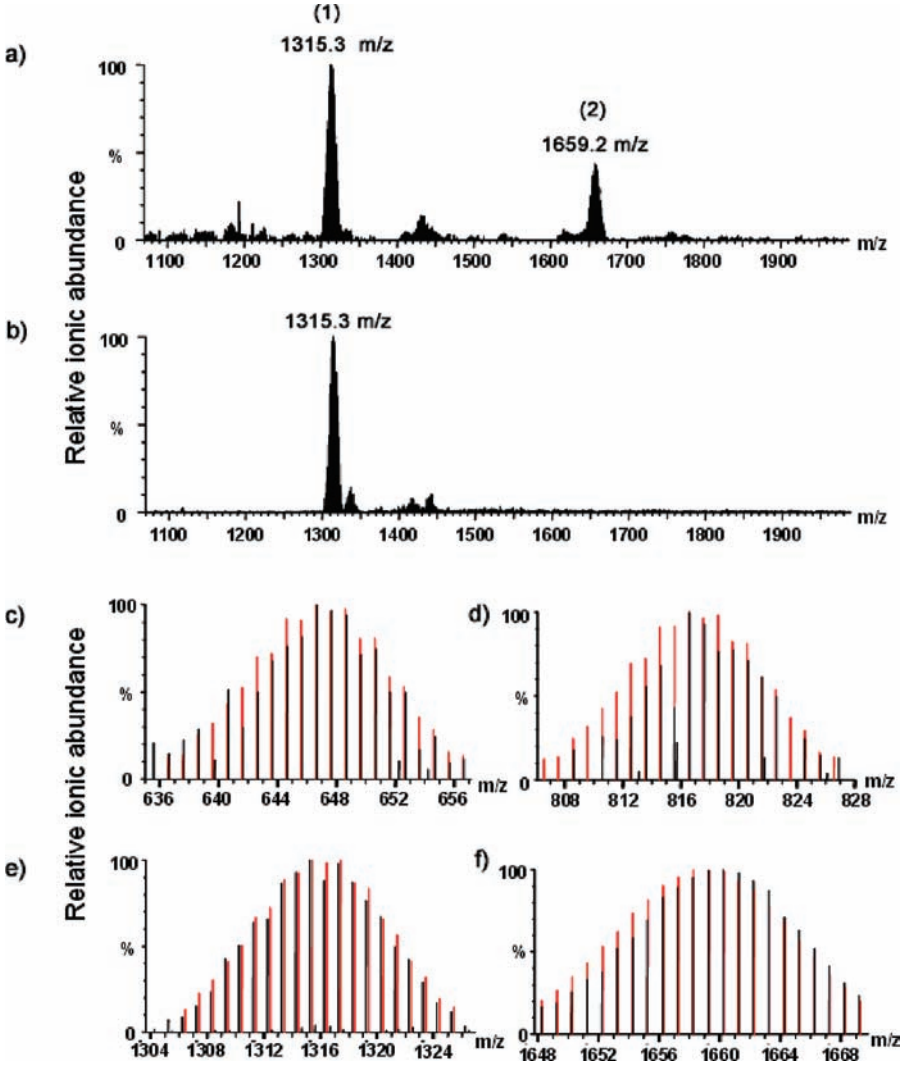

Figure 1. Negative-mode ESI-MS spectra to identify **1**: (a) reaction mixture 24 h after preparation [signal (1) centered at m/z 1315.3 corresponds to $\{H_3[Mo^V_4O_8(O_3AsC_6H_5)_4]\}^-$; signal (2) centered at m/z 1659.2 corresponds to $\{(NH_4)_2H_4[Mo^V_4Mo^{IV}_2O_{12}(OH)_3(O_3AsC_6H_5)_4]\}^-$]; (b) crystals of **1** dissolved in DMSO. (c−f) Comparison of experimental isotopic envelopes (black spectra) with simulated patterns (red spectra) for (c) $[Mo^{VI}_4O_{16}H_7]^-$ centered at m/z 646.6, (d) $\{H_9[Mo^V_4O_{14}(O_3AsC_6H_5)]\}^-$ centered at m/z 816.6, (e) $\{H_3[Mo^V_4O_8(O_3AsC_6H_5)_4]\}^-$ centered at m/z 1315.3; (f) $\{(NH_4)_2H_4[Mo^V_4Mo^{IV}_2O_{12}(OH)_3(O_3AsC_6H_5)_4]\}^-$ centered at m/z 1659.2 (cone voltage: 30 V).

cubane structure. The structure is shown in Figure 2. In this structure, the four Mo atoms are situated diagonally across from each other, occupying four corners of a cube. Four O^{2-} oxo ligands occupy the remaining four corners of the cube, and each one binds to three Mo atoms. The structure is further stabilized by four fully deprotonated PAA ligands that each bind in a μ-syn,syn bridging mode to two Mo ions, resulting in an overall octanuclear compound (the As atoms are also considered to be core atoms). The slightly distorted octahedral coordination environment of each of the four Mo ions is completed by terminal Mo=O bonds. These are situated in trans positions to the μ_3-O donors. The bond lengths of these Mo=O bonds range between 1.660(4) and 1.679(4) Å and are, as expected, significantly shorter than the Mo−μ_3-O distances [2.364(4)−2.424(4) Å].

The core structure $[Mo_4(\mu_3\text{-}O)_4]^{12+}$ deviates slightly from the geometry of an ideal cube. The Mo−O−Mo and O−Mo−O angles range between 83.82(3) and 104.04(1)° and between 76.2(4) and 89.7(4)°, respectively, differing from the ideal angle of 90°. Bond-valence-sum analysis (Supporting Information) confirms that all four Mo atoms in **1** adopt the oxidation state V+. Short Mo(1)−Mo(2) and Mo(3)−Mo(4) contacts of 2.647(1) and 2.642(1) Å, respectively, are in agreement with the assigned V+ oxidation states. The packing arrangement of the clusters **1** in the crystal structure (see the Supporting Information) is stabilized by weak hydrogen bonds between the cluster anions and constitution water molecules and NH_4^+ counterions that are situated in small channels that run in the direction of the crystallographic a axis. Structurally related cubane structures were previously isolated using squaric acid, diphenylphosphinic acid, and dimethylphosphinic acid as ligands. However, it is noteworthy that the cubane arrangement of Mo^V atoms is far less frequently observed than the structurally related rhombic planar arrangement.[11]

(11) (a) Modec, B.; Brenčič, J. V.; Burkholder, E.; Zubieta, J. *Dalton Trans.* **2003**, 4618–4625. (b) Jimtaisong, A.; Feng, L.; Sreehari, S.; Bayse, C. A.; Luck, R. L. *J. Cluster Sci.* **2008**, *19*, 181–195. (c) Schirmer, W.; Floerke, U.; Haupt, H. J. *Z. Anorg. Allg. Chem.* **1989**, *574*, 239–255.

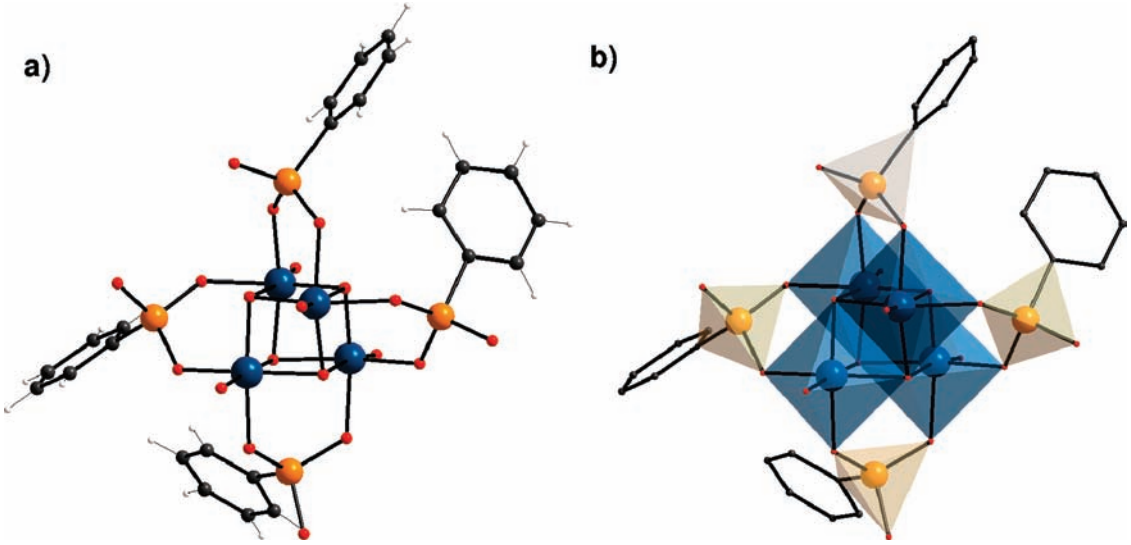

Figure 2. Crystal structure of **1** in $(NH_4)_2H_2$[**1**]$\cdot 5H_2O$: (a) ball-and-stick representation; (b) polyhedral presentation. Color code: Mo^V, blue; As, orange; O, red; C, gray; H, white. H atoms were omitted for clarity in part b.

The signal centered at m/z 1315.3 in the mass spectrum of the reaction mixture that produced **1** is in agreement with the crystallographically determined formula of the cluster anion in $(NH_4)_2H_2$[**1**]$\cdot 5H_2O$. The signal can be reproduced by recording a spectrum of pristine crystals of $(NH_4)_2H_2$[**1**]$\cdot 5H_2O$ dissolved in dimethyl sulfoxide (DMSO), further confirming that the cluster core of $(NH_4)_2H_2$[**1**]$\cdot 5H_2O$ is stable in this polar solution. Lower-molecular-mass signals in the ESI-MS spectrum centered at m/z 816.6 and 646.6 originate from the cubane cluster and can be assigned to the species $\{H_9[Mo^V_4O_{14}(O_3AsC_6H_5)]\}^-$ and $[Mo^{VI}_4O_{16}H_7]^-$, respectively. The ESI-MS spectrum of the reaction mixture further contains a high-molecular-mass signal centered at m/z 1659.2. We were able to assign this signal to a species with the formula $\{(NH_4)_2H_4[Mo^V_4Mo^{IV}_2O_{12}(OH)_3(O_3AsC_6H_5)_4]\}^-$. A closely related core structure that is stabilized by phosphonates has previously been isolated in a compound $\{Na[Mo^V_6O_{12}(OH)_3(O_3PC_6H_5)_4]_2\}^{9-}$.[12]

It can be crystallized from comparable reaction mixtures that contain alkali-metal ions, producing a solid-state structure in which two $[Mo^V_6O_{12}(OH)_3(O_3PC_6H_5)_4]^{5-}$ fragments are linked through monovalent ions (Figure 3). Within each fragment, six Mo ions form distorted octahedral coordination polyhedra, each sharing two common edges with adjacent polyhedra to form a six-membered ring. Three organic ligands are situated on the periphery of the resulting ring, each bridging two Mo ions in a μ-syn,syn-bridging mode. The tetrahedrally arranged O donors of a fourth organic ligand cap the central cavity of the ring and provide μ-O-bridging donors of three dimeric edge-sharing subunits. The aromatic moieties of the four organic ligands are arranged approximately perpendicular to the mean plane of the six-membered ring. For all of the identified species and decomposition products of **1** that originate from the reaction mixture, we successfully simulated the isotopic envelopes (Figure 1), and good fits between experimental and theoretical data further confirm our structural and constitutional assignments. The ESI-MS analysis further supports the assignment of the oxidation states and, in addition, suggests the presence of other relatively labile species in the solution. The effect of cone voltage variations on the ESI-MS spectra is shown in Figure S4 in the Supporting Information. We and others observe that higher cone voltages result in defragmentation of the coordination clusters within the spraying chamber.

Cubane complexes containing redox-active transition-metal ions represent an interesting class of compounds. Bioinorganic research approaches try to mimic the structure and reactivity of photosystem II, an enzyme that contains a $\{Mn_3Ca\}$ cubane-like core in its active site and that catalyzes the photooxidation of water to oxygen.[13a,c] Selected cubane oxo clusters show remarkable catalytic activities and redox and magnetic properties;[13c−e] they can be used as secondary building units producing microporous hybrid materials with large internal surface areas, revealing interesting sorption properties that give rise to applications as exchange/separation materials.[13f−h]

***p*-Aminophenylarsonic Acid−Mo^{VI}/Mo^V Reaction System.** Encouraged by these results, we decided to alter the ligand functionality and introduced an amino group in the para position to the arsonate functionality. When this ligand is used to control the self-assembly process upon reduction of $(NH_4)_6Mo_7O_{24}\cdot 4H_2O$, we obtain, as in the previous case, a blue solution. The ESI-MS spectrum of this reaction mixture (Figure 4) only contains one isotopic envelope in the high-mass region centered at m/z 1374.4,

(12) Khan, M. I.; Chen, Q.; Zubieta, J. *Inorg. Chim. Acta* **1995**, *235*, 135–145.

(13) (a) Brimblecombe, R.; Kolling, D. R. J.; Bond, A. M.; Dismukes, G. C.; Swiegers, G. F.; Spiccia, L. *Inorg. Chem.* **2009**, *48*, 7269–7279. (b) Betley, T. A.; Surendranath, Y.; Childress, M. V.; Alliger, G. E.; Fu, R.; Cummins, C. C.; Nocera, D. G. *Philos. Trans. R. Soc. B* **2008**, *363*, 1293–1303. (c) Demadis, K. D.; Coucouvanis, D. *Inorg. Chem.* **1994**, *33*, 4195–4197. (d) Halcrow, M. A.; Sun, J.-S.; Huffman, J. C.; Christou, G. *Inorg. Chem.* **1995**, *34*, 4167–4177. (e) Huang, J.; Mukerjee, S.; Segal, B. M.; Akashi, H.; Zhou, J.; Holm, R. H. *J. Am. Chem. Soc.* **1997**, *119*, 8662–8674. (f) Haushalter, R. C.; Strohmaier, K. G.; Lai, F. W. *Science* **1989**, *246*, 1289–1291. (g) Mundi, L. A.; Haushalter, R. C. *Inorg. Chem.* **1991**, *30*, 153–154. (h) King, H. E., Jr.; Mundi, L. A.; Strohmaier, K. G.; Haushalter, R. C. *J. Solid State Chem.* **1991**, *92*, 154–158.

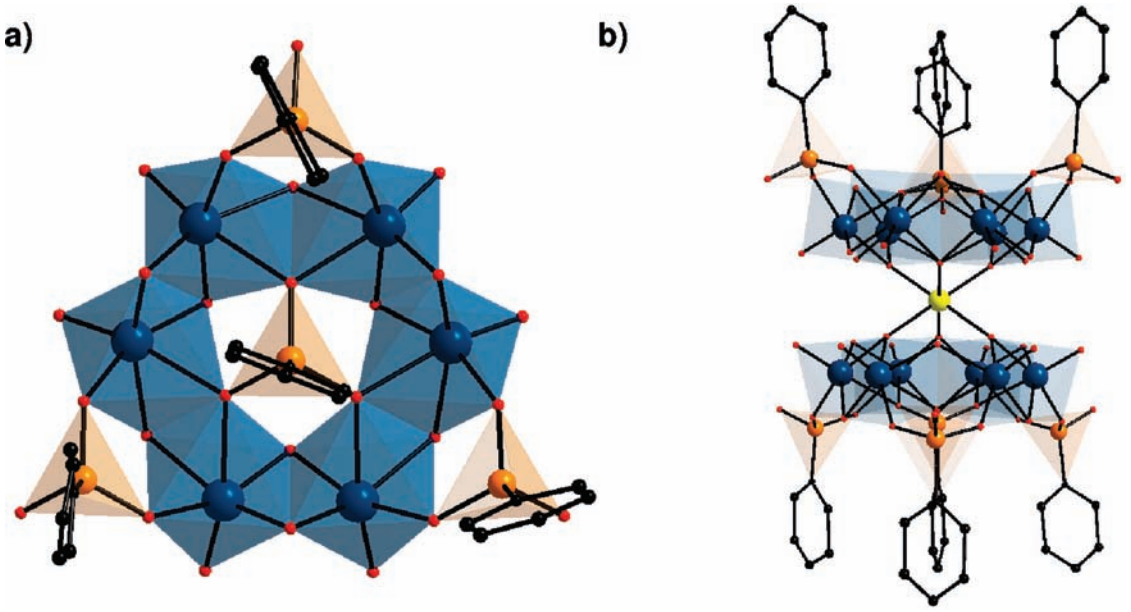

Figure 3. (a) Structure of the cluster anion $[Mo_6{}^{V}O_{12}(OH)_3(O_3PC_6H_5)_4]^{5-}$. (b) Cluster core isolated as dimeric species in which two cluster anions are linked through an alkali-metal ion.[12] Color code: Mo, blue; P, orange; O, red; C, gray; alkali metal, yellow. H atoms have been omitted for clarity.

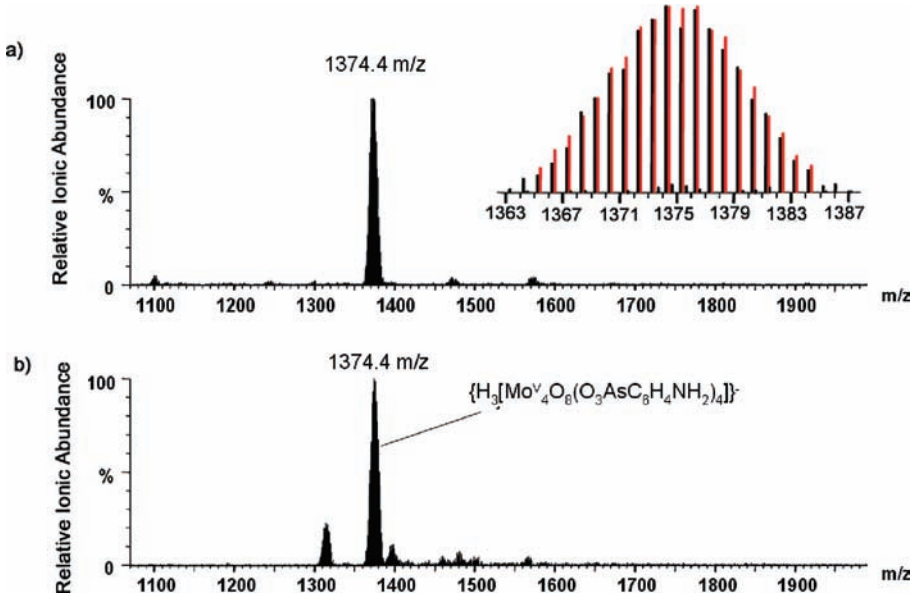

Figure 4. Negative-mode ESI-MS spectra to identify **2**: (a) reaction mixture 24 h after preparation [the signal centered at m/z 1374.4 corresponds to $\{H_3[Mo^{V}_4O_8(O_3AsC_6H_5NH_2)_4]\}^-$]; (b) crystals of **2** dissolved in DMSO. Inset: Comparison of the experimental isotopic envelopes (black spectrum) with simulated patterns (red spectrum) for **2** centered at m/z 1374.4 (cone voltage: 30 V).

corresponding to the cubane structure in $(NH_4)_2H_2$[**2**]·$DMF·4H_2O$, which crystallizes from this solution as red rod-shaped crystals. ESI-MS and NMR analyses of the isolated compound in DMSO further confirm our assignments [both $(NH_4)_2H_2$[**1**]$·5H_2O$ and $(NH_4)_2H_2$[**2**]$·DMF·4H_2O$ are insoluble in H_2O]. ESI-MS cone voltage variations are provided in the Supporting Information.

This cluster core is almost isostructural to **1**, having only slightly different structural and geometrical parameters; the bond valence sums and underlying M−O and Mo−Mo distances agree very well with those observed for **1**. The amine functionalities of the organic ligands only impose an influence on the packing arrangement of the clusters in the crystal structure, resulting in a gridlike packing arrangement, with small intercluster cavities (filled with solvent molecules) running the direction of the crystallographic *a* axis (Supporting Information).

***p*-Hydroxyphenylarsonic Acid (HPAA)−Mo^{VI}/Mo^{V} Reaction System.** Surprisingly, when HPAA is used as a stabilizing ligand under the same reaction conditions, we obtain a reaction mixture whose ESI-MS spectrum is complex and is characterized by four major isotopic envelopes centered at m/z 1377.3, 1522.2, 1704.1, and 1740.2 in the higher mass region of the spectrum (Figure 5). The signal at m/z 1377.3 can be assigned to the cubane structure, also observed in the previously examined reaction mixtures, while the high-molecular-mass signal centered at m/z 1740.2 originates from a new pentanuclear

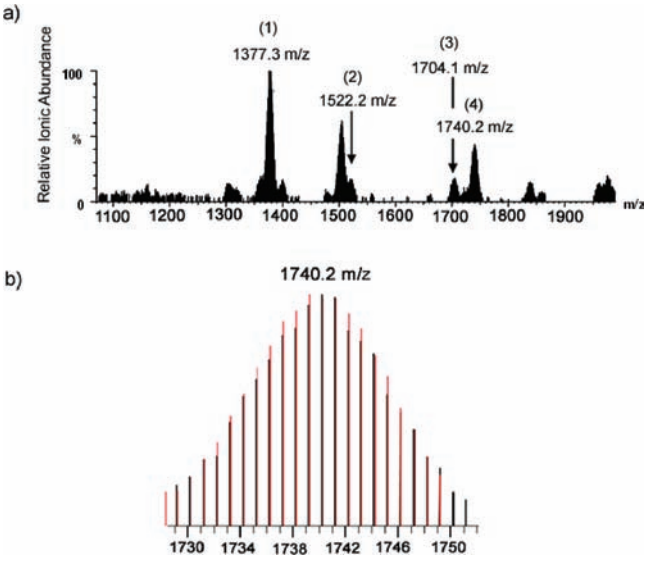

Figure 5. (a) Negative-mode ESI-MS spectra to identify **3** [reaction mixture 24 h after preparation; signal (1) at *m*/*z* 1377.3 corresponds to $\{H_3[Mo^V_4O_8(O_3AsC_6H_4OH)_4]\}^-$, signal (2) at *m*/*z* 1522.2 to $\{H_2[Mo^{VI}_2Mo^V_3O_{11}(O_3AsC_6H_4OH)_4]\}^-$, signal (3) at *m*/*z* 1704.1 to $\{(NH_4)H_3[Mo^V_6O_{12}(OH)_3(O_3AsC_6H_4OH)_4]\}^-$, and signal (4) at *m*/*z* 1740.2 to $\{H_4[Mo^{VI}_2Mo^V_3O_{11}(O_3AsC_6H_4OH)_5]\}^-$]. (b) Expanded view of the signal centered at *m*/*z* 1740.2. Comparison of the experimental isotopic envelopes (black spectrum) with simulated patterns (red spectrum) for **3** (cone voltage: 30 V).

mixed-valent Mo cluster **3**. The signal at *m*/*z* 1522.2 can be attributed to a defragmentation product of **3**, in which one organic ligand is abstracted from the cluster anion.

The ESI-MS spectrum of the reaction mixture of **3** displays a fourth signal at *m*/*z* 1704.1, which can be assigned to a hexanuclear compound $\{(NH_4)H_3[Mo^V_6O_{12}(OH)_3(O_3AsC_6H_4OH)_4]\}^-$. A similar compound was also observed during analysis of the previously described reaction systems. ESI-MS analysis including cone voltage variations (Supporting Information) clearly confirms that the tetranuclear cubane structure and the pentanuclear complex **3** form in solution in the same reaction mixture; the formation of the latter hexanuclear species might possibly be a result of processes occurring in the spraying chamber.

We succeeded in isolating **3** in $(NH_4)_5$[**3**]$\cdot 9H_2O$. The compound crystallizes as dark-blue rectangular blocks, allowing us to verify our constitutional assignment using single-crystal X-ray diffraction. $(NH_4)_5$[**3**]$\cdot 9H_2O$ contains a mixed-valent pentanuclear cluster that is stabilized by five HPAA ligands. The structure of the cluster anion is shown in Figure 6. All Mo ions in the structure are distorted octahedrally surrounded by O donors. The coordination polyhedra of Mo(1), Mo(2), Mo(3), and Mo(5) share common edges. The polyhedron of Mo(4) shares common vertices with the polyhedra of Mo(3) and Mo(5) and closes the circular entity. Four organic ligands are situated on the outer side of the ring, and each binds via its deprotonated arsonate functionalities in a μ-syn,syn-bridging mode to two Mo ions. The organic ligands bridge between Mo(2) and Mo(3), Mo(3) and Mo(4), Mo(4) and Mo(5), and Mo(5) and Mo(1), respectively. The fifth ligand is situated above the center of the $\{Mo_5\}$ ring and binds with its three O atoms to all Mo ions [O(26) binds to Mo(4) and O(3) and O(8) bridge between Mo(2) and Mo(3) and between Mo(5) and Mo(1), respectively]. The aromatic ring systems of the ligands all point in one direction and project perpendicularly to the virtual plane of the $\{Mo_5\}$ ring. The phenolic OH functionalities of the organic ligands remain protonated and are engaged in H bonds within the crystal structure. The Mo−O bond distances of Mo(3) and Mo(5) are significantly shorter than the corresponding distances of the other Mo ions in the structure. Further bond-valence-sum analyses confirm that these two Mo ions have the oxidation state VI+, while Mo(1), Mo(2), and Mo(4) are in oxidation state V+. This assignment is also in agreement with the protonation observed in the mass spectrum. The polyoxomolybdate cluster carries an overall charge of 5−, which is compensated for by NH_4^+ counterions. In the crystal structure, the cluster packs to form a layered lamellar structure with alternating inorganic and organic areas (Supporting Information).

ESI-MS studies on the crystalline material reveal that compound $(NH_4)_5$[**3**]$\cdot 9H_2O$ undergoes structural transformations when dissolved in distilled water but is stable in a DMSO environment (Supporting Information). The assignments of the oxidation states of the Mo atoms in **3** are in agreement with the observed magnetic properties of $(NH_4)_5$[**3**]$\cdot 9H_2O$. At room temperature, the χT product is 0.37 cm^3 K mol^{-1}, in good agreement with the presence of one $S = {}^1/_2$ Mo^V metal ion (expected value: 0.375 cm^3 K mol^{-1} for $g = 2$). The two other Mo^V ions appear to be magnetically silent, as expected for two spin centers that are strongly antiferromagnetically coupled ($|J| \gg 500$ K, with the Hamiltonian definition $H = -2JS_1S_2$) to give a diamagnetic dinuclear unit. Such strong antiferromagnetic exchange is common in polyoxomolybdates that feature edge- and face-sharing dinuclear molydenum octahedra.[14] When the temperature is lowered, the χT product at 1000 Oe remains constant at 0.37 cm^3 K mol^{-1} down to 1.8 K, indicating a Curie-type paramagnetism. From the Curie constant (0.37 cm^3 K mol^{-1}), the *g* value is estimated to be very close to 2. The assignment of the oxidation states is further substantiated by the observed Mo−Mo distances within **3**. The short interatomic distance of 2.574(1) Å between Mo(1) and Mo(2) is indicative for Mo−Mo bonds and in agreement with the V+ oxidation states and the observed diamagnetism. Comparable Mo^V−Mo^{VI} distances are expectedly significantly longer [Mo(1)−Mo(5) 3.359(1) Å, Mo(2)−Mo(3) 3.353(3) Å, Mo(3)−Mo(4) 3.680(2) Å, and Mo(4)−Mo(5) 3.671(5) Å]. Its mixed-valent nature distinguishes **3** from many other organoarsonate-stabilized polyoxomolybdates, which tend to exist, with few exceptions,[9a,b] predominantly in their fully oxidized forms.

4-Hydroxy-3-Nitrophenylarsonic Acid (HNPAA)−Mo^{VI}/Mo^{VI} Reaction System. We decided to investigate the influence of a disubstituted arsonate ligand on the self-assembly process of hybrid polyoxomolybdates under the same outlined reaction conditions that led to the formation of **1**−**3**. Using a substituted arsonate ligand with a hydroxyl group in the para position and a nitro group in

(14) (a) Zhang, X.; Xu, J. Q.; Yu, J. H.; Lu, J.; Xu, Y.; Chen, Y.; Wang, T. G.; Yu, X. Y.; Yang, Q. F.; Hou, Q. *J. Solid State Chem.* **2007**, *180*, 1949–1956. (b) Ma, Y.; Li, Y. G.; Wang, E. B.; Lu, Y.; Wang, X. L.; Xiao, D. R.; Xu, X. X. *Inorg. Chim. Acta* **2007**, *360*, 421–430.

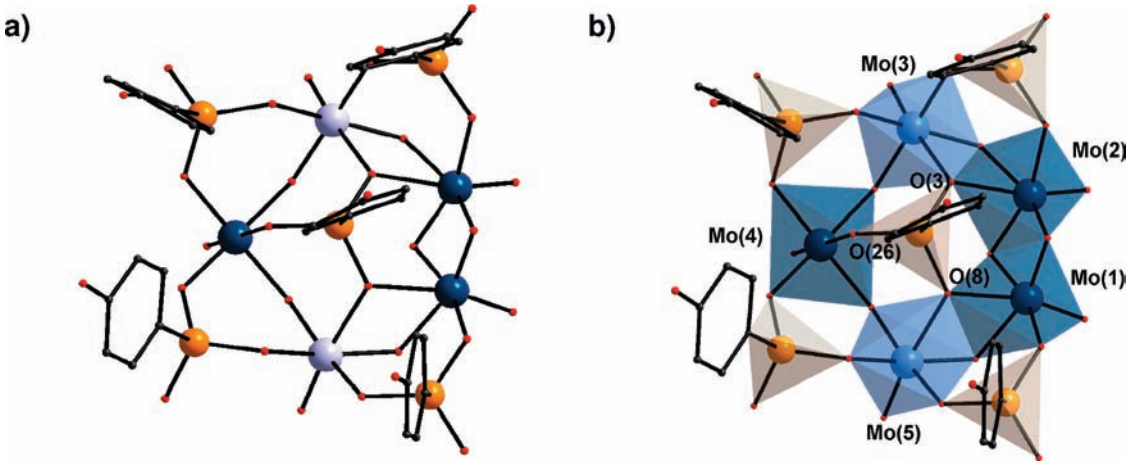

Figure 6. Crystal structure of **3** in $(NH_4)_5[\mathbf{3}]\cdot 9H_2O$: (a) ball-and-stick representation; (b) polyhedral representation of the mixed-valent pentanuclear cluster and ball-and-stick representation of the organic ligand that stabilizes **3**. Color code: Mo^{VI}, cyan; Mo^{V}, blue; As, orange; O, red; C, gray. H atoms were omitted for clarity.

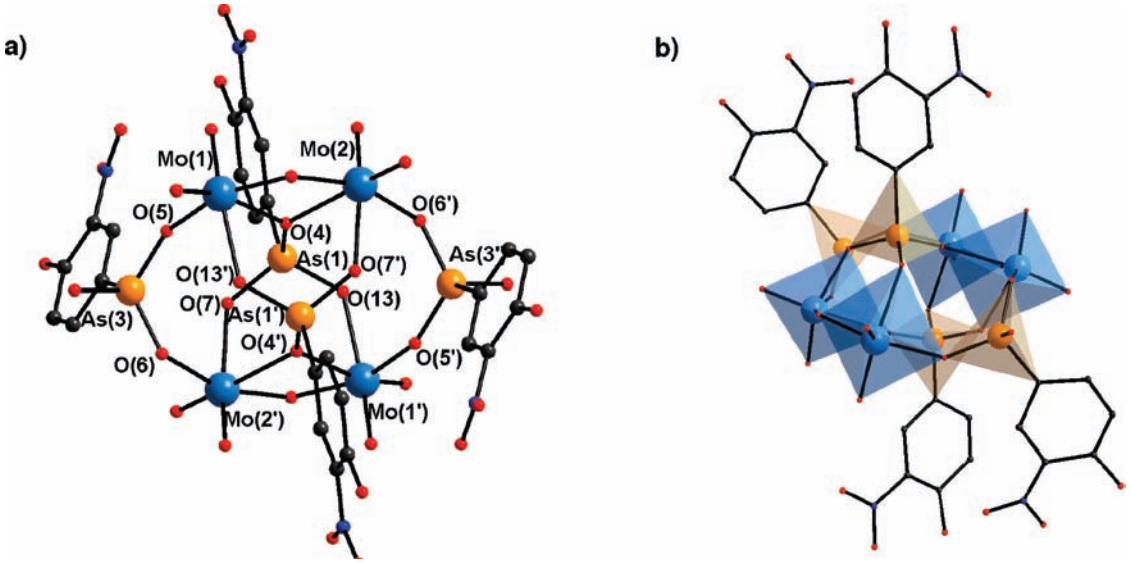

Figure 7. Crystal structure of **4** in $(NH_4)_4[\mathbf{4}]\cdot 2H_2O$: (a) ball-and-stick representation; (b) polyhedral presentation. Colro code: Mo^{VI}, cyan; As, orange; O, red; C, gray. H atoms were omitted for clarity.

the meta position, we obtain a dark-green solution, which undergoes a color change to red orange within approximately 10 days. The ESI-MS spectrum of this reaction mixture is complex, showing the presence of multiple species in the higher mass region of the spectrum. We were able to identify unambiguously the composition of one of these species. Its isotopic envelope is centered at m/z 1615.4 and corresponds to the formula of a tetranuclear molybdenum complex with the composition $\{H_9[Mo^{V}_2Mo^{IV}_2O_{10}(O_3AsC_6H_3NO_2OH)_4]\cdot H_2O\}^-$. Orange crystals of a closely related compound, $(NH_4)_4[\mathbf{4}]\cdot 2H_2O$, were obtained from the reaction mixture within a time period of 3 weeks, and single-crystal X-ray studies were performed. The core structure of **4** is related to those observed in $(Et_3NH)_4[Mo_4O_{10}(C_6H_5PO_3)_4]\cdot 2CH_3CN$ and $(Et_3NH)_4[Mo_4O_{10}(C_6H_5AsO_3)_4]\cdot 4H_2O$, respectively.[9f] The anionic cluster $[Mo^{VI}_4O_{10}(O_3AsC_6H_3NO_2OH)_4]^{4-}$ (**4**; Figure 7) contains two $\{Mo_2O_{10}\}^{8-}$ subunits in which octahedrally coordinated Mo atoms share a common edge [Mo(1)/Mo(2) and Mo(1′)/Mo(2′)]. The dimeric units are connected by four deprotonated arsonate ligands. Two of the ligands have their As atoms [As(3) and As(3′)] arranged nearly coplanar to the four Mo atoms. Each of the ligands is bridging between two Mo ions in a μ-syn,syn-bridging mode to form a six-membered $\{As_2Mo_4\}$ ring. The remaining two arsonate ligands cap both sides of the central cavity of the ring, and each provides one μ-bridging O donor [O(4) and O(4′)] of the common edges of the $\{Mo_2O_{10}\}^{8-}$ dimers. The other two O atoms of the tetrahedral arsonate functionality of each of the ligands [O(7), O(13) and O(7′), O(13′) respectively] link to the adjacent $\{Mo_2O_{10}\}^{8-}$ moiety and interconnect the dimeric subunits. The involved O donors bridge in a μ-syn,syn-bridging mode and occupy two apical positions of the octahedrally coordinated Mo atoms within the dimer units. All four Mo atoms show distorted octahedral coordination environments. Each Mo ion in **4** is involved in two short Mo=O bonds [range between 1.692(3) and 1.707(3) Å] and three elongated Mo−μ-O bonds that range between 2.276(3) and 2.427(3) Å.

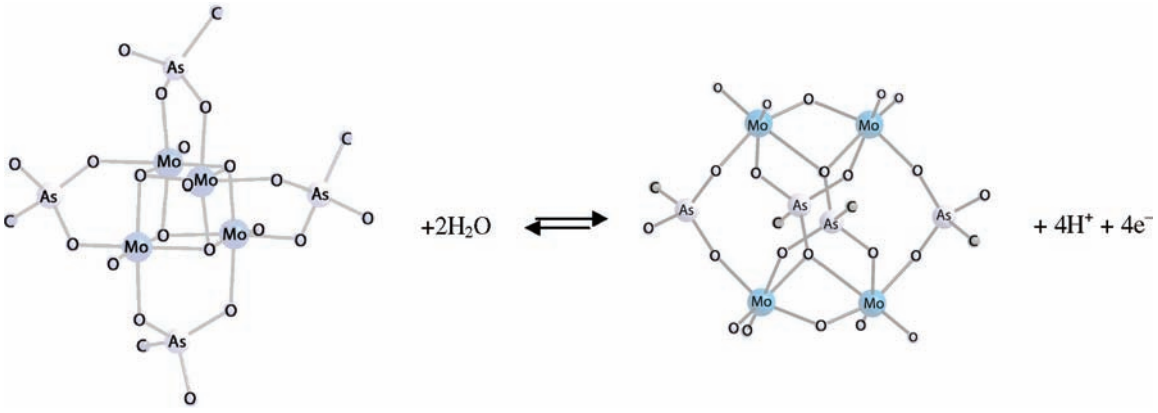

Figure 8. Formal rearrangement of the {Mo_4} core structure in **1** or **2** to give **4**.

Bond-valence-sum analyses confirm that all four Mo atoms in **4** adopt the oxidation state VI+. As expected, the disubstituted arsonate ligand imposes an influence on the self-assembly process under the investigated conditions that produce **1** and **2**. In fact, the composition of the cluster anion **4** is closely related to that of **1** and **2**. However, it seems that the OH and NO_2 functionalities of the organic ligands enforce a rearrangement of the cubane core structure. The rearrangement can formally be explained by an intramolecular condensation reaction under acidic conditions, releasing two water molecules (Figure 8). ESI-MS studies on the crystalline material reveal that **4** is unstable in solution and decomposes into inorganic or polymeric insoluble materials when dissolved in H_2O or DMSO.

The packing arrangement of the $[Mo^{VI}_4O_{10}(O_3AsC_6H_3NO_2OH)_4]^{4-}$ clusters in the crystal structure is characterized by small intercluster channels (filled with constitution water molecules and NH_4^+ counterions) that run in the direction of the crystallographic *a* axis (Supporting Information).

Further Physicochemical Characterization of the Isolated Compounds. Supplemental analyses include thermogravimetric studies, NMR, and bond-valence-sum analyses (see the Supporting Information). The thermal stabilities of all isolated compounds were investigated under a dinitrogen gas atmosphere. All compounds reveal similar decomposition behavior. The first thermogravimetric steps are the result of the loss of assigned constitution solvent molecules of the compounds and occur in a temperature range between 25 and 200 °C. Cluster degradation processes and oxidation of the organic ligands prevail in the temperature range between 200 and 600 °C. ^{1}H NMR analyses underline the stability of **1** and **2** in DMSO and are in agreement with the ESI-MS and X-ray data. The NMR spectrum of **3** is characterized by very broad signals, which are in agreement with the paramagnetic nature of the compound. Bond-valence-sum analyses confirm the assigned oxidation states of compounds **1**−**4**.

Conclusion

Our efforts focus on the application of analytical techniques that allow us to monitor and direct complex condensation reactions to produce novel functionalized hybrid materials. We report here a facile synthetic approach to functionalizing polyoxomolybdate clusters that involve the partial reduction of Mo^{VI} salts in the presence of organoarsonate ligands. We demonstrate how slight perturbations of the ligand structures can be exploited to stabilize unprecedented core structures. Our investigations underline the stability of **1**−**3** in solution, an essential requirement for potential applications as catalysts. Redox-active transition metals that adopt cubane or related structures are of particular interest to scientists because of their resemblance to active sites of enzymes, and it has recently been suggested that such oxo clusters might hold the key to catalyzing the splitting of water,[8,13a−13c] a process that might have an impact on future energy requirements providing a conceptional solution to climate issues. We demonstrate that the cubane structures **1** and **2** tolerate polar and oxophilic functional groups in the para position to the arsonate group, a characteristic that might allow the tethering of clusters to surfaces, for instance, electrodes. We have demonstrated that ESI-MS, in combination with X-ray crystallography, provides an extremely powerful tool to identify and characterize new species that form in solution. Our approach allowed us to use simple, common, well-investigated, and commercially available ligands and to screen their involvement in condensation reactions, providing us with a time-effective protocol to selectively isolate and structurally characterize a series of novel species. The effectiveness of mass spectrometry in this field science has only recently been highlighted, and our efforts extend accomplishments to complex hybrid structures. Our results underline the possibility of exploring real-time growth reactions of polyoxometales that emerge in solution, transforming from small or oligonuclear species and aggregating into large nanosized molecular clusters.

Experimental Section

All reagents were purchased from Sigma Aldrich and ABCR and used without further purification.

1: $(NH_4)_6Mo_7O_{24}\cdot 4H_2O$ (0.224 g, 0.180 mmol) and CH_3COONH_4 (0.500 g, 6.488 mmol) were dissolved under stirring in H_2O (10 mL) at room temperature, and $N_2H_4\cdot H_2SO_4$ (0.032 g, 0.244 mmol) was added as a reducing agent. Then phenylarsonic acid (PAA; 0.612 g, 3.030 mmol) was added, and the resulting reaction mixture was stirred for 10 min. Subsequently, the pH was adjusted to pH = 3.9 (20 °C) through the addition of 3.32 mL of an aqueous CH_3COOH solution (50%, v/v). After 3 weeks, red-brown crystals were collected from a dark-blue solution

Table 1. Crystal Data and Structural Refinement Parameters

	$(NH_4)_2H_2$[**1**]·$5H_2O$	$(NH_4)_2H_2$[**2**]·DMF·$4H_2O$	$(NH_4)_5$[**3**]·$9H_2O$	$(NH_4)_4$[**4**]·$2H_2O$
empirical formula	$C_{24}H_{40}As_4Mo_4N_2O_{25}$	$C_{27}H_{49}As_4Mo_4N_7O_{25}$	$C_{60}H_{126}As_{10}Mo_{10}N_{10}O_{80}$	$C_{24}H_{36}As_4Mo_4N_8O_{36}$
temperature (K)	118(2)	118(2)	108(2)	108(2)
cryst color/shape	red/triangular plate	red/rod-shaped	blue/rectangular plate	orange/rectangular plate
cryst size/mm^3	0.20 × 0.20 × 0.05	0.20 × 0.15 × 0.10	0.50 × 0.40 × 0.40	0.20 × 0.20 × 0.20
molecular mass/g mol^{-1}	1440.02	1555.16	3976.27	1696.02
cryst syst	triclinic	triclinic	triclinic	triclinic
space group	$P\bar{1}$	$P\bar{1}$	$P\bar{1}$	$P\bar{1}$
a/Å	10.009(4)	10.207(4)	19.417(4)	10.7255(19)
b/Å	15.767(5)	13.740(5)	21.040(4)	10.937(3)
c/Å	17.287(5)	19.700(8)	21.562(4)	12.000(3)
α/deg	117.09(2)	87.426(13)	113.09(3)	89.474(13)
β/deg	96.03(2)	82.265(10)	112.90(3)	66.129(10)
γ/deg	98.454(18)	71.005(11)	99.16(3)	63.926(7)
V/Å^3	2356.1(14)	2588.6(17)	6941(2)	1131.6(5)
Z	2	2	2	1
density/Mg m^{-3}	2.001	1.978	1.864	2.465
abs coeff/mm^{-1}	3.906	3.567	3.334	4.109
F(000)	1356	1494	3732	808
$2\theta_{max}$/deg	50	50	50	50.04
reflns collected	36 989	39 817	103 006	14 710
indep reflns	8303 [R(int) = 0.1174]	9114 [R(int) = 0.1044]	24429 [R(int) = 0.0648]	3987 [R(int) = 0.0313]
parameters	577	604	1587	343
S on F^2	1.036	1.006	1.059	1.036
R1, wR2 [$I > 2\sigma(I)$]	0.0985, 0.2684	0.0836, 0.1961	0.0704, 0.1844	0.0282, 0.0817
R1, wR2 (all data)	0.1171, 0.2869	0.0892, 0.2006	0.0789, 0.1930	0.0303, 0.0831

and washed with cold water. Yield: 57%. Anal. Calcd for $As_4C_{24}H_{40}Mo_4N_2O_{25}$: C, 20.01; H, 2.79; N, 1.94. Found: C, 19.65; H, 2.15; N, 1.69. FTIR (cm^{-1}): ν_{max} 2981(b), 1641(w), 1439(m), 1092(m), 966(vs), 743(vs). ^{1}H NMR (400 MHz, DMSO): δ 7.67 (m, 12H, $H^{aromatic}$), 7.97 (d, J = 7.0 Hz, 8H, $H^{aromatic}$). UV/vis (DMF): λ_{max} (ε) = 456.60 nm (1000 L mol^{-1} cm^{-1}).

2: $N_2H_4 \cdot H_2SO_4$ (0.032 g, 0.244 mmol) was added to a mixture of $(NH_4)_6Mo_7O_{24} \cdot 4H_2O$ (0.224 g, 0.180 mmol), CH_3COONH_4 (0.500 g, 6.488 mmol), H_2O (5 mL), and *N*, *N*-dimethylformamide (DMF; 5 mL). The solution was vigorously stirred for 5 min, and *p*-arsanilic acid (0.659 g, 3.030 mmol) was added. The resulting reaction mixture was further stirred for 10 min, and subsequently the pH was adjusted to pH = 4.9 (20 °C) through the addition of an aqueous CH_3COOH solution (50%, v/v). Red-brown crystals were obtained after 5−7 days. Yield: 53%. Anal. Calcd for $As_4C_{27}H_{49}Mo_4N_7O_{25}$: C, 20.85; H, 3.17; N, 6.30. Found: C, 21.14; H, 2.61; N, 6.23. FTIR (cm^{-1}): ν_{max} 3329(m), 3209(m), 1714(w), 1628(m), 1594(s), 1502(m), 1425(m), 1295(w), 1182(w), 1095(m), 958(s), 768(vs), 692(s). ^{1}H NMR (400 MHz, DMSO): δ 5.80 (s, 8H, NH_2), 6.73 (d, J = 8.5 Hz, 8H, $H^{aromatic}$), 7.56 (d, J = 8.5 Hz, 8H, $H^{aromatic}$). UV/vis (DMF): λ_{max} (ε) = 460.38 nm (1000 L mol^{-1} cm^{-1}).

3: $(NH_4)_6Mo_7O_{24} \cdot 4H_2O$ (0.224 g, 0.180 mmol) and CH_3COONH_4 (0.500 g, 6.488 mmol) were dissolved under stirring in H_2O (10 mL) at room temperature, and $N_2H_4 \cdot H_2SO_4$ (0.032 g, 0.244 mmol) was added as a reducing agent. Then HPAA (0.660 g, 3.030 mmol) was added, and the resulting reaction mixture was stirred for 10 min. Subsequently, the pH was adjusted to pH = 4.0 (20 °C) through the addition of 3.32 mL of an aqueous CH_3COOH solution (50%, v/v). Dark-blue crystals were collected after 1 week and washed with cold water. Yield: 53%. Anal. Calcd for $As_5C_{30}H_{63}Mo_5N_5O_{40}$: C, 18.12; H, 3.19; N, 3.52. Found: C, 19.03; H, 2.70; N, 3.20. FTIR (cm^{-1}): ν_{max} 2998(vbr), 1582(m), 1500(w), 1425(s), 1253(m), 1171(w), 1092(s), 944(s), 729(s). UV/vis (DMF): λ_{max} (ε) = 531.24 nm (2700 L mol^{-1} cm^{-1}).

4: The same synthetic procedure as that for $(NH_4)_2H_2$[**1**]·$5H_2O$, using HNPAA (0.797 g, 3.030 mmol) as the ligand, was used. The pH was adjusted to pH = 3.9 (20 °C) through the addition of 3.32 mL of an aqueous CH_3COOH solution (50%,v/v), and orange crystals of $(NH_4)_4[Mo_4O_{10}(O_3AsC_6H_3NO_2OH)_4] \cdot 2H_2O$ were obtained within 3 weeks. Yield: 75%. Anal. Calcd for $As_4C_{24}H_{36}Mo_4N_8O_{36}$: C, 17.00; H, 2.14; N, 6.61. Found: C, 16.52; H, 2.06; N, 5.61. FTIR (cm^{-1}): ν_{max} 3189(br), 1614(m), 1570(w), 1532(w), 1407(m), 1355(w), 1327(m), 1247(w), 1158(m), 1099(m), 940(w), 810 (vs), 762(s). ^{1}H NMR (400 MHz, DMSO): δ 6.47 (d, J = 9.0 Hz, 4H, $H^{aromatic}$), 7.17 (dd, J = 9.0 and 2.0 Hz, 4H, $H^{aromatic}$), 8.05 (d, J = 2.0 Hz, 4H, $H^{aromatic}$).

Crystallographic Data. Single-crystal analyses were performed at 150 K with a Bruker SMART APEX CCD diffractometer using graphite-monochromated Mo Kα radiation (λ = 0.710 73 Å). A full sphere of data was obtained using the ω scan method. Data were collected, processed, and corrected for Lorentz and polarization effects using *SMART* and *SAINT-NT* software.[15] The structures were solved using direct methods and refined with the *SHELXTL* program package.[16] The crystallographic data for **1**−**4** are given in Table 1. Crystallographic data, CCDC 767645−767648, can be obtained free of charge from the Cambridge Crystallographic Data Centre via www.ccdc.cam.ac.uk/data_request/cif.

Acknowledgment. The authors thank the Science Foundation Ireland (SFI) for financial support (Grants 06/RFP/CHE173 and 08/IN.1/I2047). Financial support from IRCSET (fellowship for L.Z.), the University of Bordeaux, ANR (NT09_469563, AC-MAGnets project), Région Aquitaine, GIS Advanced Materials in Aquitaine (COMET Project), and MAGMANet (NMP3-CT-2005-515767) is also gratefully acknowledged.

Supporting Information Available: Additional figures of the isolated compounds, bond-valence-sum analyses; experimental conditions for ESI-MS experiments, additional assignments,

(15) (a) *SMART*, version 5.629; Bruker-AXS Inc.: Madison, WI, 1997−2003. (b) *SAINT-Plus*, version 6.22; Bruker-AXS Inc.: Madison, WI, 1997−2003.

(16) Sheldrick, G.M. *SHELXTL*, version 5.1; Bruker AXS-Inc.: Madison, WI, 1999.

and ESI-MS cone voltage variations, analysis of the magnetic properties of $(NH_4)_5$[**3**]$\cdot 9H_2O$, powder X-ray diffraction of $(NH_4)_2H_2$[**1**]$\cdot 5H_2O$ and $(NH_4)_2H_2$[**2**]$\cdot$DMF$\cdot 4H_2O$, thermogravimetric analyses of isolated compounds, NMR spectroscopy of $(NH_4)_2H_2$[**1**]$\cdot 5H_2O$ and $(NH_4)_2H_2$[**2**]$\cdot$DMF$\cdot 4H_2O$, UV/vis spectroscopy of $(NH_4)_2H_2$[**1**]$\cdot 5H_2O$, $(NH_4)_2H_2$[**2**]$\cdot$DMF$\cdot 4H_2O$, and $(NH_4)_5$[**3**]$\cdot 9H_2O$, IR spectra of the compounds, and ORTEP diagrams of the asymmetric units of the compounds. This material is available free of charge via the Internet at http://pubs.acs.org.